Overlapping functions of YDA and MAPKKK3/MAPKKK5 upstream of MPK3/MPK6 in plant immunity and growth/development

Yidong Liu[1], Emma Leary[2], Obai Saffaf[1], R. Frank Baker[3], and Shuqun Zhang[1,#]

ORCID: 0000-0002-3401-7893 (Y.L.), 0000-0003-2080-974X (E.L.), 0000-0001-7416-6925 (O.S.), 0000-0002-2392-6338 (R.F.B), 0000-0003-2959-6461 (S.Z.)

[1] Division of Biochemistry, University of Missouri, Columbia, MO 65211, USA

[2] Division of Biological Sciences, University of Missouri, Columbia, MO 65211, USA

[3] Advanced Light Microscopy Core, University of Missouri, Columbia, MO 65211, USA

[#] Address Correspondence to: Shuqun Zhang
Tel: 573-882-5837
Fax: 573-882-5635
E-mail: Zhangsh@missouri.edu

Running title: Functions of three MAPKKKs in plant immunity and development

Key words: MAPK cascade, MPK3/MPK6, YDA, MAPKKK3/MAPKKK5, plant immunity, embryogenesis, gamete transmission

Abstract

Arabidopsis MPK3 and MPK6 play important signaling roles in plant immunity and growth/development. MKK4 and MKK5 function redundantly upstream of MPK3 and MPK6 in these processes. YDA, also known as MAPKKK4, is upstream of MKK4/MKK5 and forms a complete MAPK cascade (YDA–MKK4/MKK5–MPK3/MPK6) in regulating plant growth and development. In plant immunity, MAPKKK3 and MAPKKK5 function redundantly upstream of the same MKK4/MKK5–MPK3/MPK6 module. However, the residual activation of MPK3/MPK6 in the *mapkkk3 mapkkk5* double mutant in response to flg22 PAMP treatment suggests the presence of additional MAPKKK(s) in this MAPK cascade in signaling plant immunity. To investigate whether YDA is also involved in plant immunity, we attempted to generate *mapkkk3 mapkkk5 yda* triple mutants. However, it was not possible to recover one of the double mutant combinations (*mapkkk5 yda*) or the triple mutant (*mapkkk3 mapkkk5 yda*) due to a failure of embryogenesis. Using the CRISPR-Cas9 approach, we generated weak, N-terminal deletion alleles of *YDA*, *yda-del*, in a *mapkkk3 mapkkk5* background. PAMP-triggered MPK3/MPK6 activation was further reduced in the *mapkkk3 mapkkk5 yda-del* mutant, and the triple mutant was more susceptible to pathogen infection, suggesting YDA also plays an important role in plant immune signaling. In addition, *MAPKKK5* and, to a lesser extent, MAPKKK3 were found to contribute to gamete function and embryogenesis, together with *YDA*. While the double homozygous *mapkkk3 yda* mutant showed the same growth and development defects as the *yda* single mutant, *mapkkk5 yda* double mutant and *mapkkk3 mapkkk5 yda* triple mutants were embryo lethal, similar to the *mpk3 mpk6* double mutants. These results demonstrate that YDA, MAPKKK3, and MAPKKK5 have overlapping functions upstream of the MKK4/MKK5–MPK3/MPK6 module in both plant immunity and growth/development.

Introduction

Mitogen-activated protein kinase (MAPK) cascades are important signaling modules in all eukaryotes (Widmann et al., 1999; Ichimura et al., 2002; Zhang and Zhang, 2022). A typical MAPK cascade has at least one MAPK (or MPK), one MAPK kinase (MAPKK, also known as MKK or MEK), and one MAPKK kinase (MAPKKK, also known as MKKK or MEKK). Multiple members playing redundant or partially overlapping functions may be present at the same tier of the cascade. In response to a stimulus, the activation of MAPKKK(s), the topmost kinase(s) in a MAPK cascade, results in the phosphorylation activation of the downstream MAPKK(s). The activated MAPKK(s) then phosphorylate and activate the MAPK(s), which are capable of phosphorylating multiple downstream substrates, including transcription factors, protein kinases, other enzymes, and structural proteins, leading to a change in cellular physiology (reviewed in Ichimura et al., 2002; Pedley and Martin, 2005; Colcombet and Hirt, 2008; Meng and Zhang, 2013; Xu and Zhang, 2015; Bi and Zhou, 2017; Zhang et al., 2018; Sun and Zhang, 2022).

An increasing body of evidence has demonstrated that plant MAPK cascades are key signaling modules downstream of receptors/sensors. In plant growth and development, they function downstream of many receptor-like protein kinases (RLKs) to coordinate cellular responses to achieve normal growth and development in response to internally produced peptide ligands (reviewed in Xu and Zhang, 2015; Zhang et al., 2018; Sun and Zhang, 2022; Zhang and Zhang, 2022). Plant MAPK cascades are also key to the plant response to pathogen invasion by translating the signals generated from plant cell-surface pattern recognition receptors (PRRs) and intracellular immune receptors with nucleotide-binding and leucine-rich domains (NLRs) after sensing pathogen-derived pathogen/microbe-associated molecular patterns (P/MAMPs) and pathogen-derived effectors, respectively. In addition, plant MAPK cascades are also involved in transmitting plant-derived damage-associated molecular patterns (DAMPs) to send an early warning to other parts of the plant (Bi and Zhou, 2017; Sun and Zhang, 2022; Zhang and Zhang, 2022).

Among the 20 MAPKs in *Arabidopsis*, MPK3 and MPK6 have received the most attention because of the ease of detecting their rapid activation in response to a diverse

array of abiotic and abiotic stress-related stimuli (reviewed in Zhang and Klessig, 2001; Sun and Zhang, 2022; Zhang and Zhang, 2022). In the process of acquiring a loss-of-function system for the functional analysis of *MPK3* and *MPK6* in plant immunity, we discovered that the loss of both *MPK3* and *MPK6* genes leads to embryonic lethality. In addition, they play redundant/overlapping functions in a number of other growth and developmental processes, including stomatal development, abscission, gametogenesis, pollen guidance, inflorescence architecture, seed formation, and root development (Wang et al., 2007; Cho et al., 2008; Meng et al., 2012; Guan et al., 2014a; Guan et al., 2014b; Zhang et al., 2017; Zhu et al., 2019; Lu et al., 2020; Shao et al., 2020). Two Arabidopsis MAPKKs, MKK4 and MKK5, are upstream of MPK3/MPK6 in all these processes. YDA, also known as MAPKKK4, has been shown to be the MAPKKK in the YDA-MKK4/MKK5-MPK3/MPK6 MAPK cascade in signaling plant growth and development (reviewed in Sun and Zhang, 2022; Zhang and Zhang, 2022).

In plant immunity, MAPKKK3 and MAPKKK5 have been reported to be the upstream MAPKKKs of the MKK4/MKK5-MPK3/MPK6 module, forming a complete MAPK cascade composed of MAPKKK3/MAPKKK5-MKK4/MKK5-MPK3/MPK6 (Bi et al., 2018; Sun et al., 2018). Arabidopsis MAPKKK3 is an ortholog of tobacco MAPKKKα that has been shown to be upstream of NtMEK2 and SIPK, tobacco orthologs of MKK4/MKK5 and MPK6 in the plant hypersensitive response (HR) and pathogen resistance (del Pozo et al., 2004). These lead to the speculation that different MAPKKKs, such as YDA and MAPKKK3/MAPKKK5, might be upstream of the same MKK4/MKK5-MPK3/MPK6 module to form two separate MAPK cascades in signaling plant growth/development and immunity, respectively. However, only a partial loss of activation of MPK3/MPK6 was observed in the *mapkkk3 mapkkk5* double mutants in response to PAMPs (Bi et al., 2018; Sun et al., 2018), suggesting the existence of additional MAPKKK(s) that might be functionally redundant with MAPKKK3 and MAPKKK5 in plant immunity (Bi et al., 2018; Sun et al., 2018). In addition, the loss-of-function *yda* mutant shows weaker developmental phenotypes in comparison to the *mpk3 mpk6* double mutant. For instance, *yda* homozygous seedlings can be recovered in the progenies of *yda/+* plants (Lukowitz et al., 2004; Wang et al., 2007). In contrast, *mpk3 mpk6* double mutant cannot be recovered from the progenies of either *mpk3*

116 *mpk6/+* or *mpk3/+ mpk6* plants, and *mpk3 mpk6* double mutant embryos abort very
117 early in development (Wang et al., 2007). Together, these observations reinforce the
118 possibility that there are additional MAPKKK(s) besides YDA in the MPK3/MPK6 MAPK
119 cascade in signaling plant growth and development.
120 In this report, we demonstrate that *MAPKKK3/MAPKKK5* and *YDA* play
121 overlapping functions in both plant immunity and growth/development. Phylogenetic
122 analysis shows that YDA is closely related to MAPKKK3 and MAPKKK5 (Supplemental
123 Figure S1). They form a single unique clade in the Arabidopsis MEKK-subfamily of
124 MAPKKKs. We attempted to generate *mapkkk3 mapkkk5 yda* triple mutants using two
125 independent approaches: 1) crossing of the *mapkkk3 mapkkk5* double mutant with the
126 heterozygous *yda/+* knockout mutant; and 2) CRISPR-Cas9 knockout of *YDA* in the
127 *mapkkk3 mapkkk5* double mutant background. When the *yda* knockout mutant allele
128 (SALK_105078) was used for crossing, no *mapkkk5 yda* double or *mapkkk3 mapkkk5*
129 *yda* triple mutants were identified in the F2 and F3 generations. In contrast, *mapkkk3*
130 *yda* double mutant progenies were identified and had the same growth and
131 developmental defects as the *yda* single mutant, suggesting *MAPKKK3* plays a minimal
132 role in the process. When the CRISPR-Cas9 approach was used, we recovered only
133 *yda* weak mutant alleles with in-frame deletions (*yda-del* mutants), suggesting that
134 frame-shifting knockout mutants of *yda* in the *mapkkk3 mapkkk5* background might be
135 lethal, consistent with the results from crossing the *yda* knockout mutant and *mapkkk3*
136 *mapkkk5* double mutant. In addition to the growth/developmental phenotypes, an *yda-*
137 *del* allele (*yda-Δ42* with 42 amino acids deleted) in the *mapkkk3 mapkkk5* background
138 further compromised the activation of MPK3 and MPK6 in response to PAMP treatment
139 and plant resistance against *Pseudomonas syringae pv. tomato DC3000* (*Pst*). Based
140 on these findings, we conclude that *YDA*, *MAPPKKK3*, and *MAPKKK5* play overlapping
141 functions in both plant immunity and growth/development. Their differential contribution
142 to a specific process is hypothesized to be dependent on their levels of expression in
143 particular cells/tissues/organs.

Results

No homozygous double or triple mutant plants can be recovered from the progenies of *mapkkk5 yda/+* or *mapkkk3 mapkkk5 yda/+* plants

YDA functions upstream of MKK4/MKK5-MPK3/MPK6 to form a complete MAPK cascade in regulating a variety of plant growth and developmental processes, including embryogenesis, stomatal differentiation, and root development (reviewed in Xu and Zhang, 2015; Sun and Zhang, 2022; Zhang and Zhang, 2022). Homozygous *yda* knockout (SALK_105078) seedlings are severely dwarfed and cannot survive in soil or set seeds (Lukowitz et al., 2004; Wang et al., 2007). In the *yda* homozygous seedlings, the activation of MPK3/MPK6 in response to flg22 treatment was not compromised (Supplemental Figure S2), a likely result of the presence of *MAPKKK3* and *MAPKKK5,* which have been identified as two key MAPKKKs in the MPK3/MPK6 cascade downstream of PRRs in plant immunity (Bi et al., 2018; Sun et al., 2018). However, the residual activation of MPK3/MPK6 in the *mapkkk3 mapkkk5* double mutant also indicates the existence of additional MAPKKK(s) in the MPK3/MPK6 MAPK cascade in plant immune signaling. To determine whether YDA is also involved in the activation of MPK3/MPK6 in plant immunity, we attempted to generate a *mapkkk3 mapkkk5 yda* triple mutant by crossing the *mapkkk3 mapkkk5* double mutant with *yda/+* heterozygous plants. We envisioned that the triple mutant might be similar to the *yda* single mutant in growth and development since *mapkkk3 mapkkk5* double mutant plants have a wild-type appearance. This would allow us to recover triple homozygous mutant seedlings from the *mapkkk3 mapkkk5 yda/+* segregating population for testing the activation of MPK3/MPK6 in response to flg22 PAMP treatment.

However, no triple homozygous *mapkkk3 mapkkk5 yda* progeny could be identified in the segregating F2 population. We then screened progenies from *mapkkk3 yda/+*, *mapkkk5 yda/+*, and *mapkkk3 mapkkk5 yda/+* plants. Double homozygous *mapkkk3 yda* seedlings were identified among the progenies of *mapkkk3 yda/+* plants and were indistinguishable from *yda* in morphology (Figure 1A). In addition to a severely dwarfed stature, both *yda* and *mapkkk3 yda* seedlings had a severe stomatal clustering phenotype (Figure 1B-D). In contrast, no *mapkkk5 yda* or *mapkkk3 mapkkk5 yda*

175 seedlings could be recovered from *mapkkk5 yda/*+ or *mapkkk3 mapkkk5 yda/*+ plants,
176 suggesting potential defect(s) in either gamete transmission or embryogenesis or both.
177 We then characterized the segregation patterns by genotyping the progenies
178 from *yda/*+, *mapkkk3 yda/*+, *mapkkk5 yda/*+, and *mapkkk3 mapkkk5 yda/*+ plants. As
179 shown in Table 1, double homozygous *mapkkk3 yda* progenies were recovered from
180 the progenies of *mapkkk3 yda/*+ plants at a similar frequency as *yda* homozygous
181 seedlings from *yda/*+ plants (both were less than 25%). The reduced frequency of *yda*
182 homozygotes in either the wild-type or *mapkkk3* mutant background and the normal
183 frequencies of *yda* heterozygotes in both backgrounds suggest 1) a defect in
184 embryogenesis in *yda* homozygotes, and 2) *mapkkk3* has minimal involvement in the
185 process. The absence of *yda* homozygous seedlings in either the *mapkkk5* or *mapkkk3*
186 *mapkkk5* backgrounds suggests embryo lethality or a complete failure of male or female
187 gamete transmission. The latter was ruled out based on the reciprocal crosses detailed
188 later. In addition, the reduced frequency of heterozygous *yda* progenies in both
189 *mapkkk5* and *mapkkk3 mapkkk5* backgrounds suggests reduced transmission of either
190 the male and/or female gametes during the reproduction process, i.e. *MAPKKK5* and
191 *YDA* play overlapping functions in both gamete transmission and embryogenesis.
192
193 **Role of *YDA* and *MAPKKK5* in gamete transmission**
194 The above findings suggest a potential defect in male and/or female gamete
195 transmission. The existence of *mapkkk5 yda/*+ and *mapkkk3 mapkkk5 yda/*+ progenies
196 also supports that at least some of the male/female gametes are functional. To
197 investigate this further, we performed reciprocal crosses between *yda/*+, *mapkkk3*
198 *yda/*+, *mapkkk5 yda/*+, or *mapkkk3 mapkkk5 yda/*+ plants and Col-0 wild type. As
199 shown in Table 2, both male and female *yda* and *mapkkk3 yda* gametes were
200 transmitted at a normal frequency (~50%), suggesting that the reduced homozygous
201 *yda* and *mapkkk3 yda* progenies are a result of defective embryo development. In
202 contrast, both male and female *mapkkk5 yda* and *mapkkk3 mapkkk5 yda* gametes were
203 transmitted at reduced rates (Table 2). We then calculated that the theoretical
204 percentage of homozygous progenies should be at 15.6% and 13.7% for the *mapkkk5*
205 *yda* double and *mapkkk3 mapkkk5 yda* triple mutants, respectively, based on the

206 gamete transmission rates. Hence, the absence of viable double and triple homozygous
207 progenies suggests embryo lethality. Since *mapkkk5 yda* and *mapkkk3 mapkkk5 yda*
208 have similar frequencies in gamete transmission and both had complete embryo
209 lethality, we conclude that *MAPKKK3* plays minimal roles in these processes, and that
210 *MAPKKK5* and *YDA* function redundantly in both male and female gamete transmission
211 and embryo development. We can also conclude that *YDA* plays a more important role
212 in embryogenesis since the *yda* single mutant, but not the *mapkkk5* single mutant, has
213 an embryo development defect. In contrast, the *yda* single mutant does not show a
214 defect in gamete transmission, suggesting *MAKKK5* and *YDA* may contribute equally to
215 the process.
216
217 **Role of *YDA* and *MAPKKK5* in embryogenesis**
218 To examine embryo development, we dissected siliques from Col-0, *yda/*+,
219 *mapkkk3 yda/*+, *mapkkk5 yda/*+, and *mapkkk3 mapkkk5 yda/*+ plants. As shown in
220 Figure 2A, abnormal (shriveled or empty) seeds were observed in all genotypes except
221 Col-0 at significantly higher frequencies. In siliques from *yda/*+ and *mapkkk3 yda/*+
222 plants, seeds showed varying degrees of shrinkage. In some seeds, the embryos
223 protruded out from the seed coat (Figure 2A and 2C), a phenotype also observed in
224 *mpk6* and *mkk4 mkk5* single/double mutants (Zhang et al., 2017). In siliques from
225 *mapkkk5 yda/*+ and *mapkkk3 mapkkk5 yda/*+ plants, empty seeds, an indication of
226 aborted embryogenesis, were observed (Figures 2A and 2C). In addition, aborted
227 ovules, shown as small remnant placenta attached to the septum of the siliques, were
228 present in the siliques of *mapkkk5 yda/*+, and *mapkkk3 mapkkk5 yda/*+ plants. The
229 observation of aborted ovules is consistent with the reduced female transmission based
230 on the reciprocal cross (Table 2). In contrast to the shriveled seeds observed in the
231 siliques of *yda/*+ and *mapkkk3 yda/*+ plants, mutation of *MAPKKK5* in either *yda/*+ or
232 *mapkkk3 yda/*+ background lead to only empty seeds, suggesting that MAPKKK5 plays
233 an important role in embryogenesis. Furthermore, similar frequencies of aborted seeds
234 were observed in *mapkkk5 yda/*+ or *mapkkk3 mapkkk5 yda/*+ plants, suggesting that
235 MAPKKK3 plays a minimal role in the process.

236 Next, we cleared developing siliques collected from plants of all available
237 genotypes and observed embryos at different stages. At the 8-cell stage, *yda* and
238 *mapkkk3 yda* embryos showed suspensors of varying lengths, with some of an
239 adequate length to keep the embryo proper away from the micropyle and toward the
240 center of the endosperm; the embryo proper showed a developmental pattern closely
241 resemble the wildtype (Figure 3). In contrast, all the *mapkkk5 yda* and *mapkkk3*
242 *mapkkk5 yda* embryos had extremely short suspensors, which resulted in the embryos
243 residing in the micropylar opening and being constrained by it. At the globular stage,
244 some *yda* and *mapkkk3 yda* embryos showed a relatively normal developmental pattern
245 and were very close to the micropylar opening. As such, this class of embryos might be
246 ones eventually forced out of the seed coat to form the seeds with exposed embryos as
247 shown in Figure 2C. At the globular stage, siliques from *mapkkk5 yda/*+ and *mapkkk3*
248 *mapkkk5 yda/*+ plants had either normal-looking seeds (*YDA* or *yda/*+ genotype in
249 either a *mapkkk5* or *mapkkk3 mapkkk5* background) or empty seed coats with aborted
250 *yda* homozygous embryos in either the *mapkkk5* or *mapkkk3 mapkkk5* background. A
251 careful examination of the seeds showed remnants of the embryos in the micropylar
252 opening of the seed coat. In the subsequent stage, only empty seed coats were
253 observed, and these eventually changed to a brown color as shown in Figures 2A and
254 C. These observations reveal that all *mapkkk5 yda* and *mapkkk3 mapkkk5 yda* embryos
255 are aborted after the globular stage, while some *yda* and *mapkkk3 yda* embryos can
256 develop further and form seeds. This is consistent with the observation of reduced
257 homozygous seedlings in the progenies of *yda/*+ and *mapkkk3 yda/*+ plants and the
258 failure to recover *mapkkk5 yda* and *mapkkk3 mapkkk5 yda* mutant plants.
259
260 **Generation of weak *yda* deletion alleles using CRISPR-Cas9**
261 Because of the essential functions of *MAPKKK5* and *YDA* in embryogenesis, we
262 were unable to obtain triple knockout mutants for the analysis of their function(s) in plant
263 immunity. We then turned to the idea of generating weak *yda* deletion alleles using
264 CRISPR-Cas9. Two sites in the first exon of the *YDA* gene (Figure 4A), which encodes
265 the non-kinase domain of the *YDA* gene, were targeted in the *mapkkk3 mapkkk5* double
266 mutant background using the pYAO CRISPR-Cas9 system (Yan et al. 2015). Screening

267 of T1 plants using a pair of primers that flank the two CRISPR-Cas9 target sites allowed
268 the identification of deletion lines. They were then backcrossed to *mapkkk3 mapkkk5*
269 plants to remove the Cas9 gene. Sequencing of the region flanked by the two target
270 sites allowed the identification of multiple in-frame deletion mutant alleles (*yda-del*
271 mutant alleles, Figure 4A). However, no frame-shifting mutant allele with loss-of-function
272 *yda* was identified. Representative genotyping gel image and sequencing identification
273 of the mutants were shown in Supplemental Figure S3. We then selected an allele with
274 42-AA deletion, named *yda-Δ42*, for further analysis. The triple mutant plants (genotype:
275 *mapkkk3 mapkkk5 yda-Δ42*) had smaller stature in comparison to the *mapkkk3*
276 *mapkkk5* double mutant and Col-0 wild type (Figure 4B). It also had a stomata
277 clustering phenotype, although much less severe than that of the *yda* KO mutant
278 (Figure 4C).
279
280 **CRISPR-Cas9 deletion mutant of *YDA* further compromises the immunity of**
281 ***mapkkk3 mapkkk5* double mutant**
282 To test the activation of MPK3 and MPK6 in the *mapkkk3 mapkkk5 yda-Δ42* triple
283 mutant in the defense response, we treated seedlings with flg22 for various times and
284 collected samples to determine the phosphorylation activation of MPK3 and MPK6 in
285 Col-0, *mapkkk3 mapkkk5* double mutant, and *mapkkk3 mapkkk5 yda-Δ42* triple mutant.
286 As shown in Figure 5A, partial loss of *YDA* function in the double *mapkkk3 mapkkk5*
287 mutant background further reduced the phosphorylation activation of MPK3/MPK6 in
288 response to flg22, suggesting that YDA functions redundantly with MAPKKK3 and
289 MAPKKK5 in the process. Previously, it was shown that the double *mapkkk3 mapkkk5*
290 mutant is more susceptible to *Pseudomonas syringae pv. tomato DC3000* (*Pst*). When
291 we compared *Pst* growth in Col-0, *mapkkk3 mapkkk5*, and *mapkkk3 mapkkk5 yda-Δ42*
292 plants, we observed that the partial loss of *YDA* function further compromised plant
293 resistance against *Pst* (Figure 5B). This again demonstrated that YDA plays an
294 important role in plant immunity together with MAPKKK3 and MAPKKK5.

295 **Discussion**

296 Arabidopsis MPK3/MPK6 and their upstream MAPKKs, MKK4 and MKK5, play
297 important roles in plant immunity and growth/development. YDA has been shown to be
298 the MAPKKK upstream of MKK4/MKK5-MPK3/MPK6 to form a complete MAPK
299 cascade in plant growth and development, while MAPKKK3/MAPKKK5 function
300 upstream of MKK4/MKK5-MPK3/MPK6 in plant immunity (reviewed in Sun and Zhang,
301 2022; Zhang and Zhang, 2022). In this report, we demonstrated that YDA is also
302 involved in plant immunity together with MAPKKK3/MAPKKK5. In addition,
303 MAPKKK3/MAPKKK5, especially MAPKKK5, also play critical roles in plant growth and
304 development, together with YDA. These findings could explain why 1) there is only a
305 partial loss of MPK3/MPK6 activation in the *mapkkk3 mapkkk5* double mutant in
306 response to PAMP treatment (Supplemental Figure S2)(Bi et al., 2018; Sun et al.,
307 2018); and 2) the *yda* knockout mutant has weaker growth and developmental
308 phenotypes than the *mpk3 mpk6* double mutant (Wang et al., 2007). For instance, no
309 *mpk3 mpk6* double mutant progeny were recovered from either *mpk3 mpk6/*+ or *mpk3/*+
310 *mpk6* plants, while *yda* homozygotes were recoverable as severely dwarfed plants
311 (Figure 1A) (Lukowitz et al., 2004; Wang et al., 2007). At this stage, we cannot test the
312 defense response of the triple MAPKKK knockout mutant because of embryo lethality.
313 However, based on the further reduction of 1) MPK3/MPK6 activation in response to
314 flg22 treatment and 2) *Pst* resistance in the *mapkkk3 mapkkk5 yda-Δ42* triple mutant in
315 comparison with the *mapkkk3 mapkkk5* double mutant (Figure 5), we can conclude that
316 *YDA* also plays an important role in plant immunity.

317 The overlapping, but somewhat differential function(s) of *YDA*, *MAPKKK3*, and
318 *MAPKKK5* in plant immunity and growth/development is likely a result of their
319 differential expression patterns. The amount of MAPKKK protein present in a specific
320 type of cell/tissue/organ could determine its contribution to the signaling strength in a
321 specific biological process. Based on the Arabidopsis Atlas eFP Browser on
322 bar.utoronto.ca website (Klepikova et al., 2016), all three MAPKKKs are expressed in
323 leaves at comparable levels, making it possible for all three to contribute to plant
324 immune signaling. In contrast, *MAPKKK5* and *YDA* are expressed at much higher levels
325 in flowers than *MAPKKK3*, which could explain why the mutation of *MAPKKK3* showed

326 little impact on plant reproduction, including embryogenesis (Figures 2 and 3, Table 1)
327 and gamete transmission (Table 2) in the *yda* mutant background. Further, *mapkkk3*
328 *yda* double mutant seedlings were phenotypically identical to *yda* single mutant
329 seedlings (Figure 1). In contrast, both *MAPKKK5* and *YDA* contribute to the signaling
330 process during embryogenesis and gamete transmission, resulting in the failure to
331 recover the homozygous double mutants (*mappkkk5 yda*) or triple mutants (*mapkkk3*
332 *mapkkk5 yda*).

333 A partial loss of *YDA* function in *yda-Δ42* mutants in the *mapkkk3 mapkkk5*
334 background had a major impact on the activation of downstream MPK3/MPK6 in
335 response to flg22 treatment (Figure 5A), suggesting YDA plays an equally important
336 function as MAPKKK3 and MAPKKK5 in MPK3/MPK6 activation in plant immunity.
337 Single mutants of all three genes showed little impact on the activation of MPK3/MPK6
338 (Supplemental Figure S2) (Bi et al., 2018; Sun et al., 2018). In the double combinations,
339 the activation of MPK3/MPK6 was not decreased in *mapkkk3 yda* but was partially
340 reduced in *mapkkk3 mapkkk5* (Supplemental Figure S2) (Bi et al., 2018; Sun et al.,
341 2018). We were unable to test the *mapkkk5 yda* double or *mapkkk3 mapkkk5 yda* triple
342 knockout plants because of their embryo lethality. MPK3/MPK6 activation is very rapid
343 in response to PAMP treatment, suggesting the preexistence of a protein complex in
344 MAPK signaling. At this stage, the factor(s) involved in the formation of this putative
345 complex in plant MAPK signaling is largely unknown. Because of the presence of large
346 extensions in the N- and/or C-termini of the MAPKKKs, there is a possibility that they
347 function as scaffolds to hold MAPKK(s) and MAPK(s) in the MAPK cascade together as
348 in the mammalian MEKK1, also a large protein with binding sites for other components
349 of the MAPK cascade (Pearson et al., 2001). The kinase domain of YDA resides in the
350 middle of the protein (amino acid residues 400 to 656 out of the 883 total amino acids).
351 Small deletions in the first 150-AA region (Figure 4A) is unlikely to affect the activity of
352 the kinase domain directly. Further reduction of MPK3/MPK6 activation observed in the
353 *mapkkk3 mapkkk5 yda-Δ42* triple mutant in comparison to the *mapkkk3 mapkkk5*
354 double mutant (Figure 5A) is likely a result of a reduced functionality of the non-kinase
355 domain of YDA in the MAPK cascade, for instance in its interaction with either upstream

356 components such as RLCKs or downstream MAPKKs/MAPKs. Further research is
357 needed to define the functional domains of this large MAPKKK in *Arabidopsis*.
358 It is possible that, when one or two MAPKKK genes are mutated, the remaining
359 member(s) can maintain a complex with MAPKK(s) and MAPK(s) to sustain a normal or
360 close-to-normal activation of MPK3/MPK6 and the downstream signaling process. In
361 this scenario, compromised activation of downstream MAPK(s) occur only when the
362 total amount of MAPKKK protein drops below a threshold needed to maintain the
363 signaling strength. In the various biological processes, these three MAPKKKs may have
364 differential contributions because of their differential express patterns. With respect to
365 plant immunity, *mapkkk3 mapkkk5* double mutant starts to show compromised
366 MPK3/MPK6 activation and disease resistance, and partial loss of *yda* function in the
367 *mapkkk3 mapkkk5* background (Figure 5) leads to further reduction in the plant immune
368 response. It is likely that triple *mapkkk3 mapkkk5 yda* knockout mutation might have no
369 MPK3/MPK6 activation after PAMP treatment. However, we cannot test this at this
370 stage because of the embryo lethality. In plant embryogenesis, the *yda* single mutant
371 leads to severe phenotype, but is still viable. In contrast, the loss of *mapkkk5* on top of
372 *yda* results in complete failure of embryogenesis. In this process, *YDA* plays a more
373 important role than *MAPKKK5* because single *mapkkk5* mutant does not have
374 embryogenesis defect. However, in male/female gamete transmission, neither *yda* nor
375 *mapkkk5* mutant has a phenotype, but the double mutant gametes show reduced
376 transmission (Table 2), suggesting that YDA and MAPKKK5 might contribute equally to
377 the process.
378 YDA was first identified as a MAPKKK involved in embryogenesis and stomatal
379 differentiation (Bergmann et al., 2004; Lukowitz et al., 2004). Later, YDA was placed
380 upstream of the MKK4/MKK5–MPK3/MPK6 module in a variety of
381 growth/developmental processes, including stomatal differentiation, embryogenesis,
382 inflorescence architecture, and root development (Wang et al., 2007; Bayer et al., 2009;
383 Meng et al., 2012; Smekalova et al., 2014; Ueda et al., 2017; Lu et al., 2020; Shao et
384 al., 2020). This MAPK cascade (YDA–MKK4/MPK5–MPK3/MPK6) is a key signaling
385 module downstream of ER/ERLs receptors in plant growth and development (reviewed
386 in Sun and Zhang, 2022; Zhang and Zhang, 2022). Recently, several studies have

387 implicated *YDA* in plant immunity but with contradictory results. It was reported that
388 plant resistance to pathogens was compromised in weak *yda* mutant alleles, and that
389 plants expressing the constitutively active YDA protein showed broad-spectrum
390 resistance to fungi, bacteria, and oomycetes with different colonization modes (Sopena-
391 Torres et al., 2018). Furthermore, ER/ERLs receptors are upstream of the YDA–
392 MKK4/MKK5–MPK3/MPK6 MAPK cascade in a shared signaling pathway in plant
393 immunity and stomatal formation. Tomato orthologs of Arabidopsis *YDA* were also
394 shown to play a positive role in disease resistance (Tellez et al., 2020). However, in
395 another study using RNAi suppression of *YDA*, it was concluded that *YDA* and
396 *MAPKKK3/MAPKKK5* interact antagonistically in plant development and immunity (Sun
397 et al., 2018). Of particular note, the developmental defects caused by the silencing of
398 *YDA* were suppressed in the double *mapkkk3 mapkkk5* mutant. As well, *YDA* gene
399 silencing enhanced the activation of MPK3 and MPK6 after PAMP treatment,
400 suggesting a negative role for *YDA* in the plant immune response.
401 Our conclusion in this report is that YDA, MAPKKK3, and MAPKKK5 have
402 overlapping functions in both plant immunity and growth/development. All three
403 MAPKKKs function as positive regulators upstream of MPK3/MPK6 in the same MAPK
404 cascade (Figure 6). It is likely that they contribute differentially to the activation of
405 MPK3/MPK6 and the downstream events in different biological processes, dependent
406 on their expression levels in specific cells/tissues/organs. MPK3 and MPK6 have been
407 shown to be downstream of a variety of plant receptors/sensors in plant
408 growth/development and immunity (reviewed in Sun and Zhang, 2022; Zhang and
409 Zhang, 2022). The sensing of either external cues or internally produced ligands by
410 these receptors leads to the activation of MPK3 and MPK6 through the upstream
411 MKK4/MKK5 MAPKKs and YDA/MAPKKK3/MAPKKK5 MAPKKKs, which in turn
412 activates events/responses further downstream in plant growth/development and
413 immunity.

414 **Materials and Methods**

415

416 **Plant materials and growth conditions**

417 Mutant and wild-type plants of the *Arabidopsis thaliana* Columbia (Col-0) ecotype
418 were used in all experiments. A T-DNA insertion mutant of *YDA* was obtained from the
419 Arabidopsis Biological Resource Center (ABRC, https://abrc.osu.edu; SALK_105078;
420 Alonso et al., 2003) and previously described (Wang et al., 2007). The double *mapkkk3-*
421 *2 mapkkk5-2* mutant was kindly provided by Dr. Jian-Min Zhou (Bi et al., 2018). Seeds
422 were plated on half-strength Murashige and Skoog medium with 0.45% PhytoAgar after
423 surface sterilization and imbibing at 4°C for 3 days. Plates were incubated in a tissue
424 culture chamber at 22°C under continuous light (50 μE m^{-2} s^{-1}) for 5 - 7 days. Seedlings
425 were then transplanted into soil and grown in a growth chamber with a 14-h light/10-h
426 dark cycle (100 μE m^{-2} s^{-1}) unless stated otherwise.

427

428 **Generation of *yda* deletion mutant alleles using CRISPR-Cas9**

429 The CRISPR/Cas9 construct was prepared by inserting two *YDA* sgRNA into a
430 pYAO:hSpCas9 vector as described previously (Yan et al., 2015). After transformation
431 into the *mapkkk3-2 mapkkk5-2* double mutant plants (Bi et al., 2018), T1 *yda* deletion
432 mutants in *mapkkk3 mapkkk5* background were identified by PCR genotyping. Cas9-
433 free T3 homozygous mutant individuals were identified, and the T4 generation was used
434 for experiments.

435

436 **Observation of embryos, seeds, and stomata**

437 For Nomarski microscopy of cleared seeds, siliques with embryos at the 8-cell
438 and globular stages were collected from flowering plants and cleared for 2 h in 0.5 mL
439 of clearing solution (Herr, 1971). Cleared siliques were examined using a Leica DM
440 5500B microscope equipped with Nomarski optics. Siliques with seeds after the bent-
441 cotyledon stage were dissected and imaged using a Panasonic digital camera.
442 Defective seeds at the maturation stage were selected under a dissecting microscope
443 and imaged using a Leica M205 FA stereomicroscope. Stomata on the leaf surface

444 were observed and imaged using an Olympus microscope with a digital camera
445 attachment.
446
447 **Protein extraction and immunoblot analysis**
448 Protein extraction and immunoblot were carried out as previously described (Su
449 et al., 2018). Total proteins (10 μg) were separated on 10% SDS-PAGE gel. For better
450 separation, electrophoresis was continued for another 15 min after the blue tracking dye
451 came out of the gel. Phosphorylation activation of MPK3 and MPK6 was detected by
452 using anti-pTEpY (Cell signaling, dilution 1:5,000). After incubation with primary
453 antibodies and washing, the blots were incubated with horseradish peroxidase-
454 conjugated goat-anti-rabbit IgG secondary antibodies (Sigma, dilution 1:10,000), and
455 the bands were visualized using an enhanced chemiluminescence kit (Perkin Elmer)
456 according to the manufacturer's instructions.
457
458 **Pathogen inoculation and disease resistance assay**
459 *Pseudomonas syringae pv. tomato* (*Pst*) *DC3000* inoculation and disease
460 resistance assays were performed as previously described (Su et al., 2018). *Pst* was
461 grown overnight at 28°C on Pseudomonas Agar (Difco Laboratories) with Rif (50
462 μg/mL). Four-week-old Col-0 and mutant plants grown under a short-day light cycle (10
463 h of light and 14 h of dark) were infiltrated with *Pst* (OD600 = 0.0005 in 10 mM $MgCl_2$).
464 Pathogen growth was determined three days post-inoculation (DPI).
465
466 **Quantification and statistical analysis**
467 At least three independent repetitions were performed. Data from one of the
468 independent repetitions with similar results are shown in the figures. Statistical analysis
469 of the experiments is detailed in the figure legends. GraphPad Prism was used for
470 statistical analyses. One-way ANOVA or two-way ANOVA analysis with Tukey's post-
471 hoc test was performed to evaluate whether the differences were statistically significant.
472 Lower case letters above the columns were used to indicate differences that are
473 statistically significant with p-values indicated in figure legends.
474

475 **Accession Numbers**

476 Sequence data from this article can be found in the TAIR database
477 (https://www.arabidopsis.org) under the following accession numbers: AT1G63700
478 (YDA or MAPKKK4), AT1G53570 (MAPKKK3 or MAPKKKα), and AT5G66850
479 (MAPKKK5).

Acknowledgements

We thank Dr. Jian-Min Zhou (Institute of Genetics and Developmental Biology, Chinese Academy of Sciences) for providing the *mapkkk3-2 mapkkk5-2* double mutant seeds. This research was supported by a grant from the National Science Foundation to S.Z. (Award 1856093).

Author contributions

S.Z. and Y.L. designed the project. Y.L., E.L., O.S., R.F.B., and S.Z. performed the experiments. Y.L. and S.Z. analyzed the results and wrote the manuscript.

Competing interests

The authors declare no competing financial interest.

494 **Supporting Information**

495 Additional Supporting Information may be found in the online version of this article.

496

497 **Supplemental Figure S1:** Phylogenetic analysis of the MEKK subgroup of all putative
498 Arabidopsis MAPKKKs.

499

500 **Supplemental Figure S2:** Activation of MPK3/MPK6 in various *mapkkk* mutant
501 seedlings after flg22 treatment.

502

503 **Supplemental Figure S3:** Genotyping and sequencing identification of *yda-Δ42* mutant
504 allele generated using CRISPR-Cas9.

505

506 **Supplemental Table 1.** Primers used in this study.

507 **References**

508 **Bayer, M., Nawy, T., Giglione, C., Galli, M., Meinnel, T., and Lukowitz, W.** (2009)
509 Paternal control of embryonic patterning in *Arabidopsis thaliana*. Science **323:**
510 1485-1488.

511 **Bergmann, D.C., Lukowitz, W., and Somerville, C.R.** (2004) Stomatal development
512 and pattern controlled by a MAPKK kinase. Science **304:** 1494-1497.

513 **Bi, G., and Zhou, J.M.** (2017) MAP kinase signaling pathways: A hub of plant-microbe
514 interactions. Cell Host Microbe **21:** 270-273.

515 **Bi, G., Zhou, Z., Wang, W., Li, L., Rao, S., Wu, Y., Zhang, X., Menke, F.L.H., Chen,**
516 **S., and Zhou, J.M.** (2018) Receptor-like cytoplasmic kinases directly link diverse
517 pattern recognition receptors to the activation of mitogen-activated protein kinase
518 cascades in *Arabidopsis*. Plant Cell **30:** 1543-1561.

519 **Cho, S.K., Larue, C.T., Chevalier, D., Wang, H., Jinn, T.L., Zhang, S., and Walker,**
520 **J.C.** (2008) Regulation of floral organ abscission in *Arabidopsis thaliana*. Proc.
521 Natl. Acad. Sci. U.S.A. **105:** 15629-15634.

522 **Colcombet, J., and Hirt, H.** (2008) Arabidopsis MAPKs: a complex signalling network
523 involved in multiple biological processes. Biochem. J. **413:** 217-226.

524 d**el Pozo, O., Pedley, K.F., and Martin, G.B.** (2004) MAPKKKalpha is a positive
525 regulator of cell death associated with both plant immunity and disease. EMBO J.
526 **23:** 3072-3082.

527 **Guan, Y., Lu, J., Xu, J., McClure, B., and Zhang, S.** (2014a) Two mitogen-activated
528 protein kinases, MPK3 and MPK6, are required for funicular guidance of pollen
529 tubes in *Arabidopsis*. Plant Physiol. **165:** 528-533.

530 **Guan, Y., Meng, X., Khanna, R., LaMontagne, E., Liu, Y., and Zhang, S.** (2014b)
531 Phosphorylation of a WRKY transcription factor by MAPKs is required for pollen
532 development and function in *Arabidopsis*. PLoS Genet. **10:** e1004384.

533 **Herr, J.M.J.** (1971) A new clearing-squash technique for the study of ovule
534 development in angiosperms. Ameri. J. Bot. **58:** 780-790.

535 **Ichimura, K., Shinozaki, K., Tena, G., Sheen, J., Henry, Y., Champion, A., Kreis, M.,**
536 **Zhang, S., Hirt, H., Wilson, C., Heberle-Bors, E., Ellis, B.E., Morris, P.C.,**
537 **Innes, R.W., Ecker, J.R., Scheel, D., Klessig, D.F., Machida, Y., Mundy, J.,**
538 **Ohashi, Y., and Walker, J.C.** (2002) Mitogen-activated protein kinase cascades
539 in plants: a new nomenclature. Trends Plant Sci. **7:** 301-308.

540 **Klepikova, A.V., Kasianov, A.S., Gerasimov, E.S., Logacheva, M.D., and Penin,**
541 **A.A.** (2016) A high resolution map of the *Arabidopsis thaliana* developmental
542 transcriptome based on RNA-seq profiling. Plant J. **88:** 1058-1070.

543 **Lu, X., Shi, H., Ou, Y., Cui, Y., Chang, J., Peng, L., Gou, X., He, K., and Li, J.** (2020)
544 RGF1-RGI1, a peptide-receptor complex, regulates Arabidopsis root meristem
545 development via a MAPK signaling cascade. Mol. Plant **13:** 1594-1607.

546 **Lukowitz, W., Roeder, A., Parmenter, D., and Somerville, C.** (2004) A MAPKK kinase
547 gene regulates extra-embryonic cell fate in *Arabidopsis*. Cell **116:** 109-119.

548 **Meng, X,. Wang, H., He, Y., Liu, Y., Walker, J.C., Torii, K.U., and Zhang, S.** (2012) A
549 MAPK cascade downstream of ERECTA receptor-like protein kinase regulates
550 Arabidopsis inflorescence architecture by promoting localized cell proliferation.
551 Plant Cell **24:** 4948-4960.

552 **Meng, X., and Zhang, S.** (2013) MAPK cascades in plant disease resistance signaling.
553 Ann. Rev. Phytopathol. **51:** 245-266.

554 **Pearson, G., Robinson, F., Beers Gibson, T., Xu, B.E., Karandikar, M., Berman, K.,**
555 **and Cobb, M.H.** (2001) Mitogen-activated protein (MAP) kinase pathways:
556 regulation and physiological functions. Endocr. Rev. **22:** 153-183.

557 **Pedley, K.F., and Martin, G.B.** (2005) Role of mitogen-activated protein kinases in
558 plant immunity. Cur. Opin. Plant Biol. **8:** 541-547.

559 **Shao, Y., Yu, X., Xu, X., Li, Y., Yuan, W., Xu, Y,. Mao, C., Zhang, S., and Xu, J.**
560 (2020) The YDA-MKK4/MKK5-MPK3/MPK6 cascade functions downstream of
561 the RGF1-RGI ligand-receptor pair in regulating mitotic activity in root apical
562 meristem. Mol. Plant **13:** 1608-1623.

563 **Smekalova, V., Luptovciak, I., Komis, G., Samajova, O., Ovecka, M., Doskocilova,**
564 **A., Takac, T., Vadovic, P., Novak, O., Pechan, T., Ziemann, A., Kosutova, P.,**
565 **and Samaj, J.** (2014) Involvement of YODA and mitogen activated protein
566 kinase 6 in Arabidopsis post-embryogenic root development through auxin up-
567 regulation and cell division plane orientation. New Phytol. **203:** 1175-1193.

568 **Sopena-Torres, S., Jorda, L., Sanchez-Rodriguez, C., Miedes, E., Escudero, V.,**
569 **Swami, S., Lopez, G., Pislewska-Bednarek, M., Lassowskat, I., Lee, J., Gu,**
570 **Y., Haigis, S., Alexander, D., Pattathil, S., Munoz-Barrios, A., Bednarek, P.,**
571 **Somerville, S., Schulze-Lefert, P., Hahn, M.G., Scheel, D., and Molina, A.**
572 (2018) YODA MAP3K kinase regulates plant immune responses conferring
573 broad-spectrum disease resistance. New Phytol. **218:** 661-680.

574 **Su, J., Yang, L., Zhu, Q., Wu, H., He, Y., Liu, Y., Xu, J., Jiang, D., and Zhang, S.**
575 (2018) Active photosynthetic inhibition mediated by MPK3/MPK6 is critical to
576 effector-triggered immunity. PLoS Biol. **16:** e2004122.

577 **Sun, T., Nitta, Y., Zhang, Q., Wu, D., Tian, H., Lee, J.S., and Zhang, Y.** (2018)
578 Antagonistic interactions between two MAP kinase cascades in plant
579 development and immune signaling. EMBO Rep. **19:** e45324.

580 **Sun, T., and Zhang, Y.** (2022) MAP kinase cascades in plant development and
581 immune signaling. EMBO Rep. **23:** e53817.

582 **Tellez, J., Munoz-Barrios, A., Sopena-Torres, S., Martin-Forero, A.F., Ortega, A.,**
583 **Perez, R., Sanz, Y., Borja, M., de Marcos, A., Nicolas, M., Jahrmann, T.,**
584 **Mena, M., Jorda, L., and Molina, A.** (2020) YODA kinase controls a novel
585 immune pathway of tomato conferring enhanced disease resistance to the
586 bacterium *Pseudomonas syringae*. Front. Plant Sci. **11:** e584471.

587 **Ueda, M., Aichinger, E., Gong, W., Groot ,E., Verstraeten, I., Vu, L.D., De Smet, I.,**
588 **Higashiyama, T., Umeda, M,. and Laux, T.** (2017) Transcriptional integration of
589 paternal and maternal factors in the Arabidopsis zygote. Genes Dev. **31:** 617-
590 627.

591 **Wang, H., Ngwenyama, N., Liu, Y., Walker, J.C., and Zhang, S.** (2007) Stomatal
592 development and patterning are regulated by environmentally responsive
593 mitogen-activated protein kinases in *Arabidopsis*. Plant Cell **19:** 63-73.

594 **Widmann, C., Gibson, S., Jarpe, M.B., and Johnson, G.L.** (1999) Mitogen-activated
595 protein kinase: Conservation of a three-kinase module from yeast to human.
596 Physiol Rev. **79:** 143-180.

597 **Xu, J., and Zhang, S.** (2015) Mitogen-activated protein kinase cascades in signaling
598 plant growth and development. Trends Plant Sci. **20:** 56-64.

599 **Yan, L., Wei, S., Wu, Y., Hu, R., Li, H., Yang, W., and Xie, Q.** (2015) High-efficiency
600 genome editing in *Arabidopsis* using YAO promoter-driven CRISPR/Cas9
601 system. Mol. Plant **8:** 1820-1823.

602 **Zhang, M., Su, J., Zhang, Y., Xu, J., and Zhang, S.** (2018) Conveying endogenous
603 and exogenous signals: MAPK cascades in plant growth and defense. Curr.
604 Opin. Plant Biol. **45:** 1-10.

605 **Zhang, M., Wu, H., Su, J., Wang, H., Zhu, Q., Liu, Y., Xu, J., Lukowitz, W., and**
606 **Zhang, S.** (2017) Maternal control of embryogenesis by MPK6 and its upstream
607 MKK4/MKK5 in *Arabidopsis*. Plant J. **92:** 1005-1019.

608 **Zhang, M., and Zhang, S.** (2022) Mitogen-activated protein kinase cascades in plant
609 signaling. J. Integr. Plant Biol. **64:** 301-341.

610 **Zhang, S., and Klessig, D.F.** (2001) MAPK cascades in plant defense signaling.
611 Trends Plant Sci. **6:** 520-527.

612 Z**hu, Q., Shao, Y., Ge, S., Zhang, M., Zhang, T., Hu, X., Liu, Y., Walker, J., Zhang,**
613 **S., and Xu, J.** (2019) A MAPK cascade downstream of IDA-HAE/HSL2 ligand-
614 receptor pair in lateral root emergence. Nature Plants **5:** 414-423.

615

616 **Figure legends**

617

618 **Figure 1: Phenotypes of *yda* single and *mapkkk3 yda* double mutant seedlings.**
619 (**A**) Dwarf phenotype of homozygous *yda* single and *mapkkk3 yda* double mutant
620 seedlings. Fourteen-day-old seedlings from progenies of *yda/*+ single and *mapkkk3*
621 *yda/*+ double plants were imaged. The genotypes were confirmed by PCR and caps
622 markers. Size bar: 1 cm. (**B**-**D**) The stomatal patterning of Col-0 (B), *yda* (C), and
623 *mapkkk3 yda* (D) seedlings was observed under an Olympus camera with digital
624 camera. Size bars: 25 μm.

625

626 **Figure 2: Aborted/abnormal seeds and ovules in the single, double, and triple**
627 ***mapkkk* mutants.**
628 (**A**) Siliques with embryos matured beyond the bend-cotyledon stage were split open
629 from the side to reveal the seeds inside. Representative abnormal/aborted seeds are
630 indicated by arrowheads, aborted ovules by arrows, and seeds with exposed embryos
631 by asterisks. Size bar: 3 mm. (**B**) Aborted ovules, normal seeds, and abnormal/aborted
632 seeds in each silique were counted, and their percentages calculated. Two-way ANOVA
633 analysis with Tukey's post-hoc test was performed to determine if the differences were
634 significant ($n \geq 6$). Different lowercase letters indicate significant differences among
635 different genotypes ($P < 0.01$) (**C**) Shriveled/exposed or aborted seeds were collected
636 and imaged under a dissecting microscopy with a digital camera system. Size bars: 0.5
637 mm.

638

639 **Figure 3: Defective embryo development of *yda*, *mapkkk3 yda*, *mapkkk5 yda*, and**
640 ***mapkkk3 mapkkk5 yda* mutants.**
641 Siliques with embryos at the 8-cell and globular stages were collected from *yda/*+,
642 *mapkkk3 yda/*+, *mapkkk5 yda/*+, or *mapkkk3 mapkkk5 yda/*+ plants. After clearing, the
643 embryos were imaged with DIC on a Leica Microscope. Size bars: 50 μm.

644

645 **Figure 4: Weak *yda* mutant alleles generated using CRISPR-Cas9 in a *mapkkk3***
646 ***mapkkk5* background have weak *yda* phenotype.**

647 (**A**) A CRISPR-Cas9 construct containing two sgRNAs targeting two different sites in the
648 N-terminal region of *YDA* was used to generate deletion *yda* mutant alleles in the
649 *mapkkk3 mapkkk5* double mutant background. PCR genotyping was used to identify
650 deletion mutant alleles and subsequent sequencing of PCR fragments revealed the
651 nature of these mutations. Translated amino acid sequences were aligned to the wild-
652 type YDA sequence. Blue bars above the sequence indicate the corresponding position
653 of the two sgRNA target sites. Numbers indicate the beginning and ending AA positions
654 of the wild-type YDA protein. All mutant alleles identified are in-frame deletion alleles
655 (*yda-del*). Some had substitutions of a few amino acids (marked in red color). Mutant
656 alleles with a 42-amino acid deletion (*yda-Δ42*) were the most common and were used
657 for experiments. **(B)** Dwarf stature of the *yda-Δ42* mutant plants. Four-week-old Col-0,
658 *mapkkk3 mapkkk5*, and *mapkkk3 mapkkk5 yda-Δ42* plants grown under 14h light : 10h
659 dark cycle were imaged. Size bar: 2 cm. (**C**) Stomatal clustering in the *yda-Δ42* mutant.
660 The epidermis of twelve-day-old Col-0, *mapkkk3 mapkkk5*, or *mapkkk3 mapkkk5 yda-*
661 *Δ42* seedlings was observed. Size bars: 25 μm.
662
663 **Figure 5: Compromised MPK3/MPK6 activation and pathogen resistance in the**
664 ***mapkkk3 mapkkk5 yda-Δ42* triple mutant.**
665 (**A**) MPK3/MPK6 activation triggered by flg22 is further reduced in the *mapkkk3*
666 *mapkkk5 yda-Δ42* triple mutant seedlings. Fourteen-day-old Col-0, *mapkkk3 mapkkk5*
667 double, and *mapkkk3 mapkkk5 yda-Δ42* triple mutant seedlings were treated with flg22
668 (30 nM final concentration) and collected at the indicated time. The phosphorylation
669 activation of MPK3 and MPK6 were detected by using anti-pTEpY antibody. An equal
670 amount of total protein (10 μg) was loaded in each lane, as confirmed by CBB staining
671 of duplicate gels. (**B**) Four-week-old Col-0, *mapkkk3 mapkkk5*, and *mapkkk3 mapkkk5*
672 *yda-Δ42* plants were infiltration-inoculated with *Pst* (OD_{600} = 0.0005). Inoculated amount
673 and bacterial growth were measured at 0 and 3 dpi, respectively. Values are means ±
674 SD, n = 5. Lower-case letters above the bars indicate significantly different groups (one-
675 way ANOVA, $P < 0.01$).
676

677 **Figure 6: Overlapping functions of YDA, MAPKKK3, and MAPKKK5 in the**
678 **MPK3/MPK6 MAPK cascade in signaling plant immunity and growth/development.**
679 Plant perception of either exogenously derived PAMPs such as flg22 or endogenously
680 produced peptide ligands such as epidermal factors (EPFs) and EPF-likes (EPFLs) by
681 plant pattern-recognition receptors (PRRs, such as FLS2) and other RLK receptors
682 such as ERECTA (ER) and ER-likes (ERLs) activate the MPK3/MPK6 MAPK cascade.
683 MKK4 and MKK5, two redundant MAPKKs, function upstream of MPK3/MPK6. Three
684 MAPKKKs including YDA, MAPKKK3, and MAPKKK5 play overlapping, yet differential,
685 functions in the MPK3/MPK6 cascade. Depending on the levels of their expression in
686 different cells/tissues/organs, they show differential functions in plant immunity and
687 growth/development upstream of MKK4/MKK5–MPK3/MPK6 in a variety of biological
688 processes.

689 **Table 1**. Segregation ratios of *YDA* gene in the progenies of *yda/+*, *mapkkk3 yda/+*,
690 *mapkkk5 yda/+*, and *mapkkk3 mapkkk5 yda/+* plants.
691

Genotypes	**Total**	***YDA***	***yda/+***	***yda***
yda/+	106	24.5%	62.3%	13.2%
mapkkk3 yda/+	104	27.9%	60.5%	11.5%
mapkkk5 yda/+	101	42.6%	57.4%	0.0%
mapkkk3 mapkkk5 yda/+	206	45.4%	54.6%	0.0%

692
693 Note: Seeds collected from *yda/+*, *mapkkk3 yda/+*, *mapkkk5 yda/+*, and *mapkkk3*
694 *mapkkk5 yda/+* plants were sterilized using bleach and sown on MS plates after
695 imbibition at 4 ºC for 3 days. Fourteen-day-old seedlings were collected for PCR
696 genotyping.

697 **Table 2**. Transmission rates of the *yda* mutant gamete in different backgrounds (wild
698 type, *mapkkk3*, *mapkkk5*, or *mapkkk3 mapkkk5*) based on reciprocal crosses
699

Genotype (Female x Male)	**Genotype of F1 progenies**		**TE of *yda* gamete (%)**
	yda/+	***YDA***	
Col-0 ♀ x *yda/+* ♂	64	70	47.8
***yda/+* ♀ x Col-0 ♂**	83	67	55.3
Col-0 ♀ x *mapkkk3 yda/+* ♂	67	76	46.9
***mapkkk3 yda/+* ♀ x Col-0 ♂**	66	60	52.4
Col-0 ♀ x *mapkkk5 yda/+* ♂	58	98	37.2
***mapkkk5 yda/+* ♀ x Col-0 ♂**	62	86	41.9
Col-0 ♀ x *mapkkk3 mapkkk5 yda/+* ♂	50	89	36.0
***mapkkk3 mapkkk5 yda/+* ♀ x Col-0 ♂**	54	88	38.0

700
701 Note: Plants with *yda/+*, *mapkkk3 yda/+*, *mapkkk5 yda/+*, and *mapkkk3 mapkkk5 yda/+*
702 genotypes were crossed with Col-0 wild type as either male or female. After bleach
703 sterilization and imbibition at 4 ºC for 3 days, the F1 seeds were sown on MS plates.
704 Fourteen-day-old seedlings were collected for PCR genotyping. TE: transmission
705 efficiency.
706

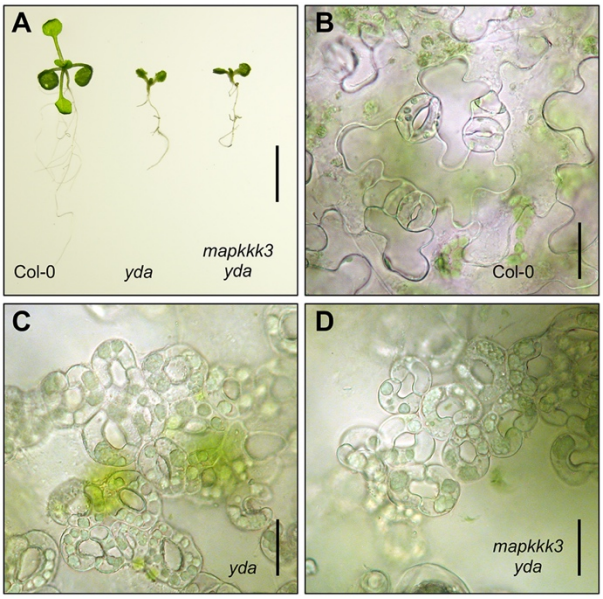

Figure 1: Phenotypes of *yda* single and *mapkkk3 yda* double mutant seedlings. (**A**) Dwarf phenotype of homozygous *yda* single and *mapkkk3 yda* double mutant seedlings. Fourteen-day-old seedlings from progenies of *yda/+* single and *mapkkk3 yda/+* double plants were imaged. The genotypes were confirmed by PCR and caps markers. Size bar: 1 cm. (**B**-**D**) The stomatal patterning of Col-0 (B), *yda* (C), and *mapkkk3 yda* (D) seedlings was observed under an Olympus camera with digital camera. Size bars: 25 µm.

716

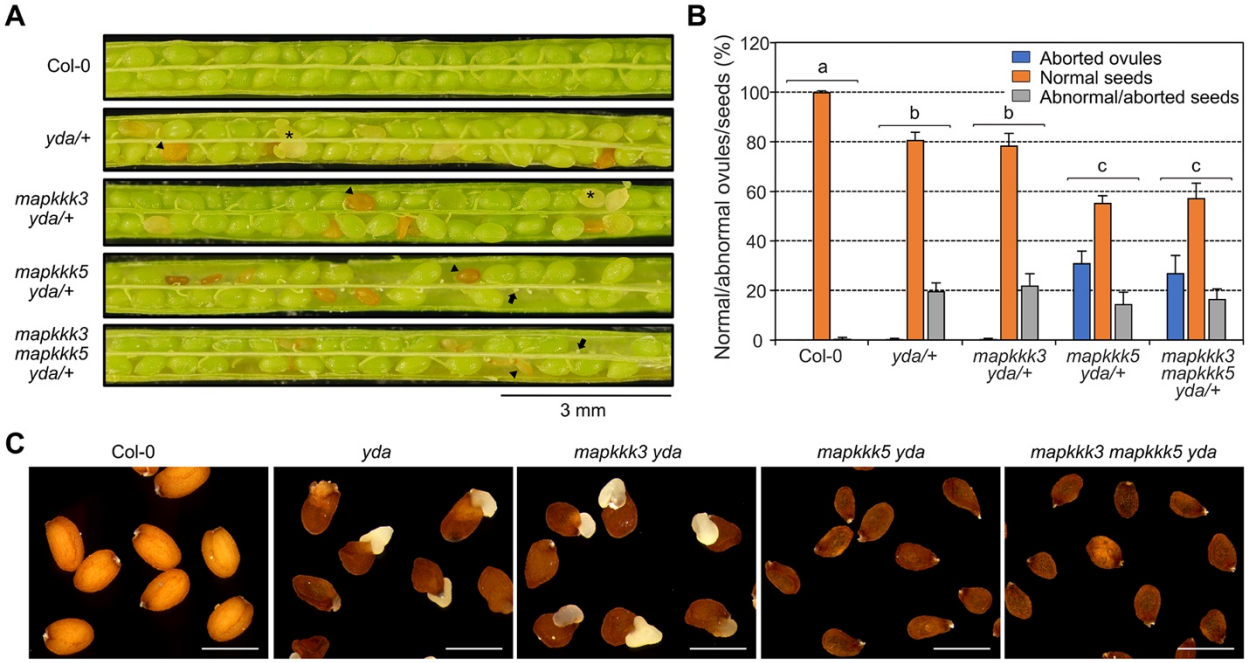

717

718

719 **Figure 2: Aborted/abnormal seeds and ovules in the single, double, and triple**
720 ***mapkkk* mutants.**
721 (**A**) Siliques with embryos matured beyond the bent-cotyledon stage were split open
722 from the side to reveal the seeds inside. Representative abnormal/aborted seeds are
723 indicated by arrowheads, aborted ovules by arrows, and seeds with exposed embryos
724 by asterisks. Size bar: 3 mm. (**B**) Aborted ovules, normal seeds, and abnormal/aborted
725 seeds in each silique were counted, and their percentages calculated. Two-way ANOVA
726 analysis with Tukey's post-hoc test was performed to determine if the differences were
727 significant ($n \geq 6$). Different lowercase letters indicate significant differences among
728 different genotypes ($P < 0.01$) (**C**) Shriveled/exposed or aborted seeds were collected
729 and imaged under a dissecting microscopy with a digital camera system. Size bars: 0.5
730 mm.

731

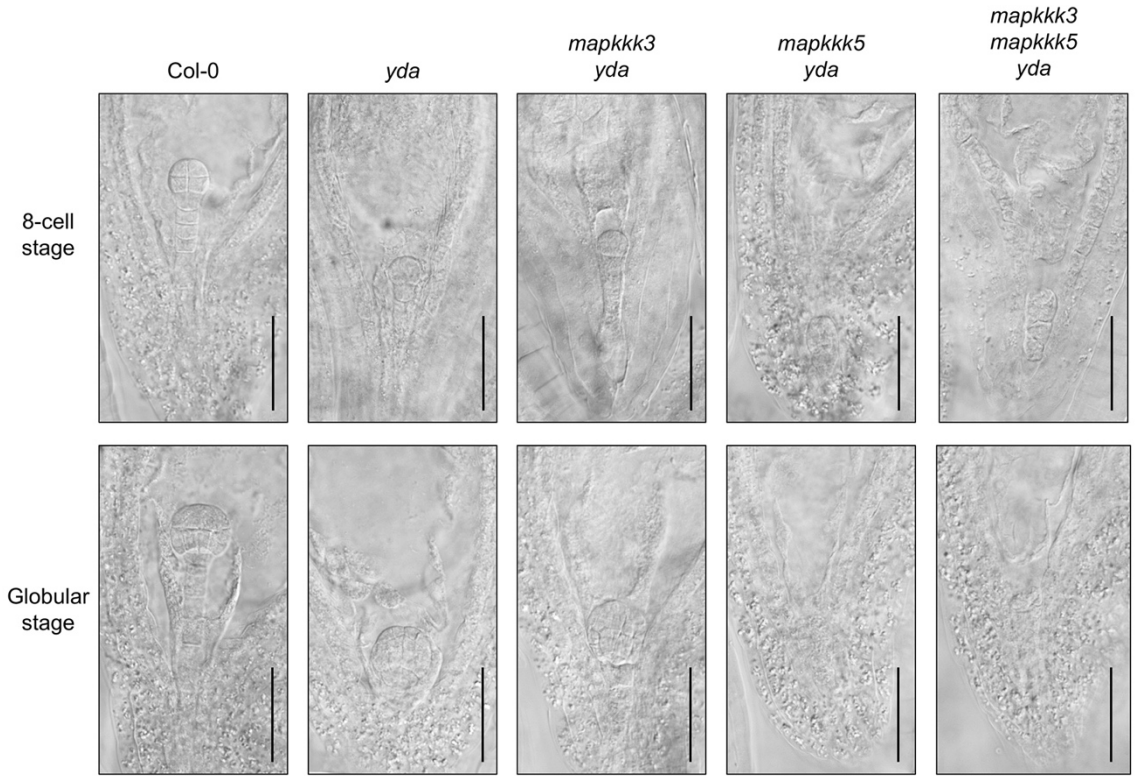

732
733
734 **Figure 3: Defective embryo development of *yda*, *mapkkk3 yda*, *mapkkk5 yda*, and**
735 ***mapkkk3 mapkkk5 yda* mutants.**
736 Siliques with embryos at the 8-cell and globular stages were collected from *yda/*+,
737 *mapkkk3 yda/*+, *mapkkk5 yda/*+, or *mapkkk3 mapkkk5 yda/*+ plants. After clearing, the
738 embryos were imaged with DIC on a Leica microscope. Size bars: 50 µm.

739

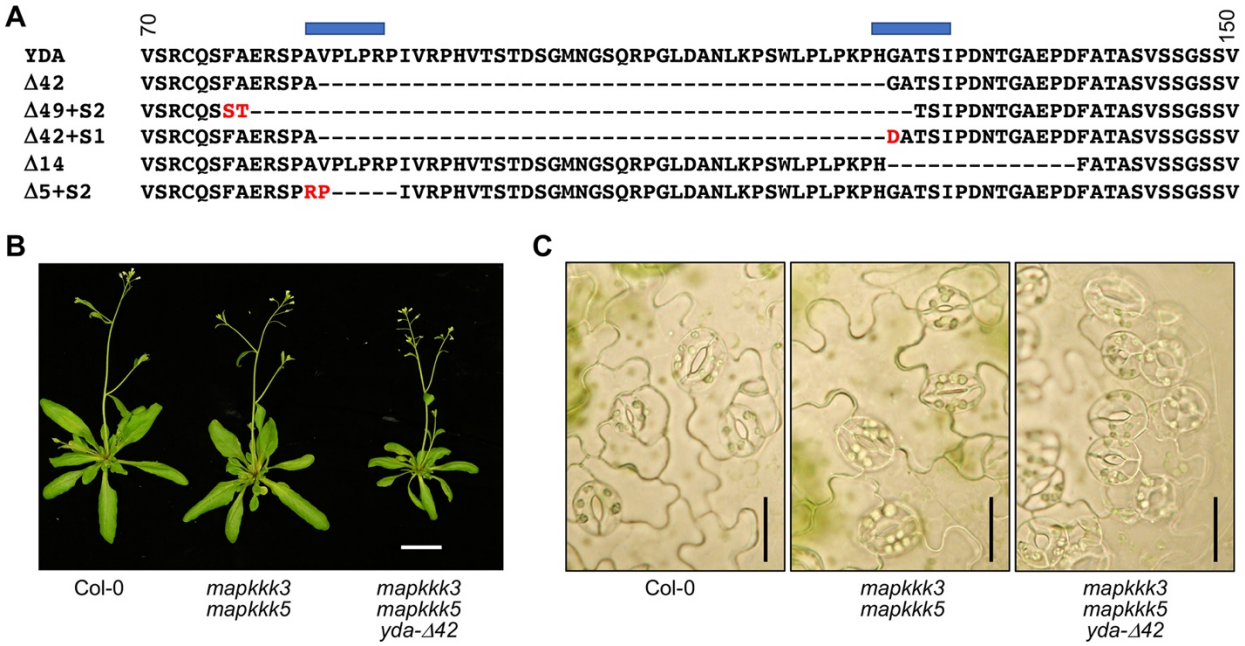

740

741

742 **Figure 4: Weak *yda* mutant alleles generated using CRISPR-Cas9 in a *mapkkk3***
743 ***mapkkk5* background have weak *yda* phenotype.**
744 (**A**) A CRISPR-Cas9 construct containing two sgRNAs targeting two different sites in the
745 N-terminal region of *YDA* was used to generate deletion *yda* mutant alleles in the
746 *mapkkk3 mapkkk5* double mutant background. PCR genotyping was used to identify
747 deletion mutant alleles and subsequent sequencing of PCR fragments revealed the
748 nature of these mutations. Translated amino acid sequences were aligned to the wild-
749 type YDA sequence. Blue bars above the sequence indicate the corresponding position
750 of the two sgRNA target sites. Numbers indicate the beginning and ending AA positions
751 of the wild-type YDA protein. All mutant alleles identified are in-frame deletion alleles
752 (*yda-del*). Some had substitutions of a few amino acids (marked in red color). Mutant
753 alleles with a 42-amino acid deletion (*yda-Δ42*) were the most common and were used
754 for experiments. **(B)** Dwarf stature of the *yda-Δ42* mutant plants. Four-week-old Col-0,
755 *mapkkk3 mapkkk5*, and *mapkkk3 mapkkk5 yda-Δ42* plants grown under 14h light : 10h
756 dark cycle were imaged. Size bar: 2 cm. (**C**) Stomatal clustering in the *yda-Δ42* mutant.
757 The epidermis of twelve-day-old Col-0, *mapkkk3 mapkkk5*, or *mapkkk3 mapkkk5 yda-*
758 *Δ42* seedlings was observed. Size bars: 25 µm.

759

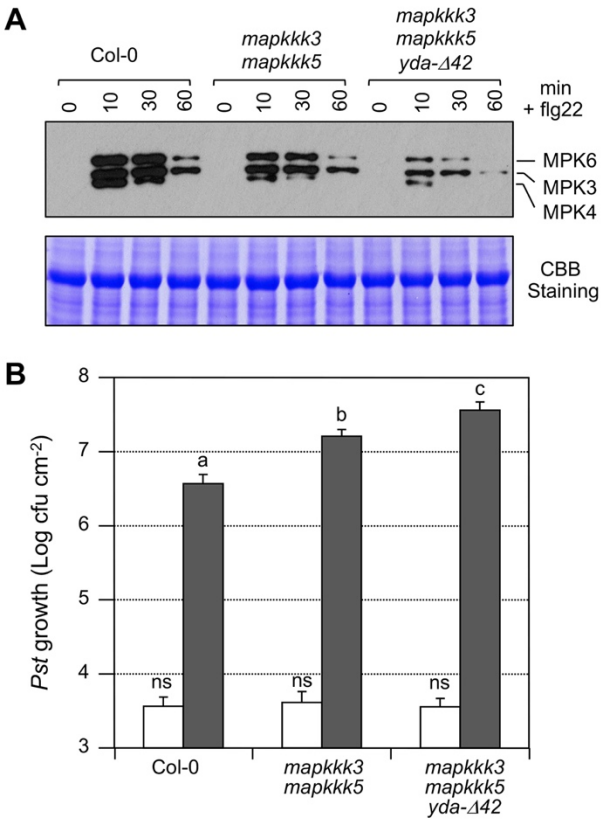

760
761

762 **Figure 5: Compromised MPK3/MPK6 activation and pathogen resistance in the**
763 ***mapkkk3 mapkkk5 yda-Δ42* triple mutant.**
764 (**A**) MPK3/MPK6 activation triggered by flg22 is further reduced in the *mapkkk3*
765 *mapkkk5 yda-Δ42* triple mutant seedlings. Fourteen-day-old Col-0, *mapkkk3 mapkkk5*
766 double, and *mapkkk3 mapkkk5 yda-Δ42* triple mutant seedlings were treated with flg22
767 (30 nM final concentration) and collected at the indicated time. The phosphorylation
768 activation of MPK3 and MPK6 were detected by using anti-pTEpY antibody. An equal
769 amount of total protein (10 µg) was loaded in each lane, as confirmed by CBB staining
770 of duplicate gels. (**B**) Four-week-old Col-0, *mapkkk3 mapkkk5*, and *mapkkk3 mapkkk5*
771 *yda-Δ42* plants were infiltration-inoculated with *Pst* (OD_{600} = 0.0005). Inoculated amount
772 and bacterial growth were measured at 0 and 3 dpi, respectively. Values are means ±
773 SD, n = 5. Lower-case letters above the bars indicate significantly different groups (one-
774 way ANOVA, $P < 0.01$).

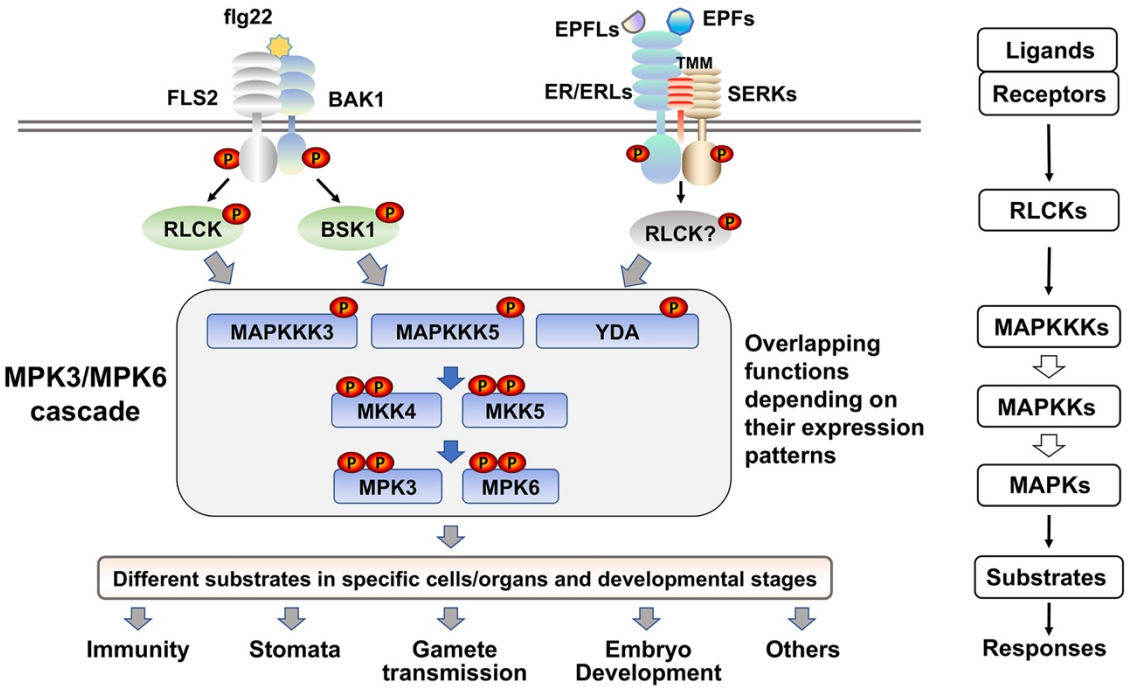

Figure 6: Overlapping functions of YDA, MAPKKK3, and MAPKKK5 in the MPK3/MPK6 MAPK cascade in signaling plant immunity and growth/development. Plant perception of either exogenously derived PAMPs such as flg22 or endogenously produced peptide ligands such as epidermal factors (EPFs) and EPF-likes (EPFLs) by plant pattern-recognition receptors (PRRs, such as FLS2) and other RLK receptors such as ERECTA (ER) and ER-likes (ERLs) activate the MPK3/MPK6 MAPK cascade. MKK4 and MKK5, two redundant MAPKKs, function upstream of MPK3/MPK6. Three MAPKKKs including YDA, MAPKKK3, and MAPKKK5 play overlapping, yet differential, functions in the MPK3/MPK6 cascade. Depending on the levels of their expression in different cells/tissues/organs, they show differential functions in plant immunity and growth/development upstream of MKK4/MKK5–MPK3/MPK6 in a variety of biological processes.

790 **Supplemental Figures**

791

792

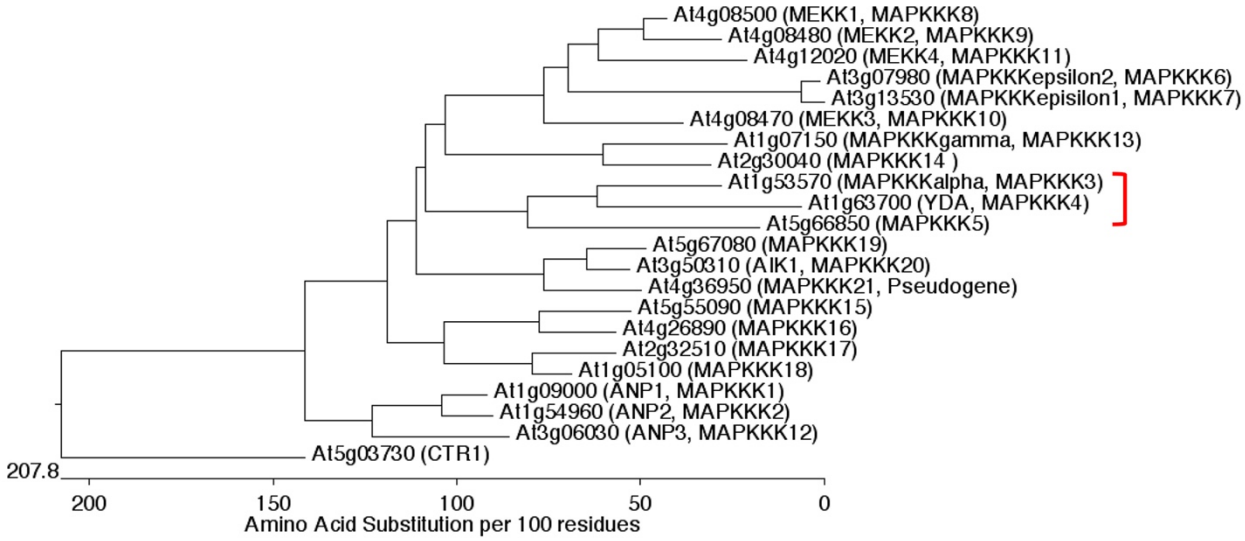

793

794 **Supplemental Figure S1: Phylogenetic analysis of the MEKK subgroup of putative**
795 **Arabidopsis MAPKKKs.**
796 The phylogenetic tree was generated using the Clustal W method (MegaAlign program
797 of DNAStar). Amino acid sequences were used for alignment. Arabidopsis CTR1, a
798 member of the Raf-like putative MAPKKKs, was used as an anchor. In addition to the
799 gene codes, the common names used in publications and systematic names
800 (https://www.arabidopsis.org/browse/genefamily/MAPKKK.jsp) are included in
801 parentheses. Red bracket indicates the YDA/MAPKKK3/MAPKKK5 group.

802
803

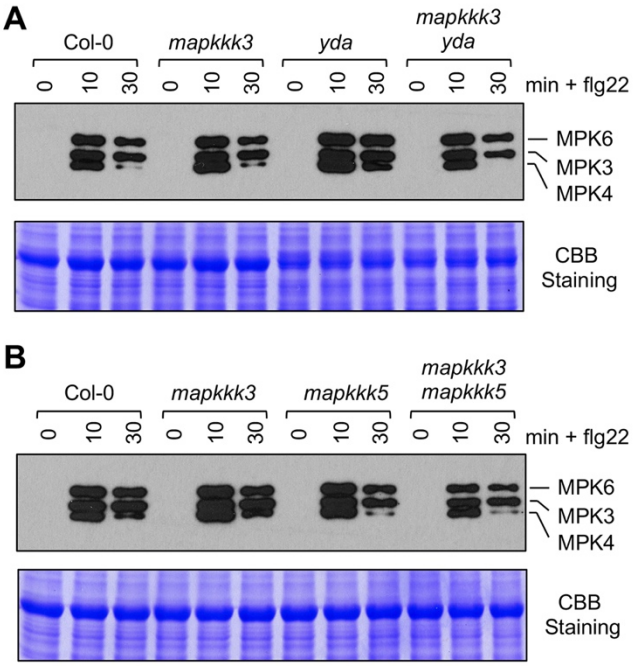

804

805 **Supplemental Figure S2: Activation of MPK3/MPK6 in various *mapkkk* mutant**
806 **seedlings after flg22 treatment.**
807 (**A**) MPK3/MPK6 activation in response to flg22 treatment is not reduced in *yda* single,
808 *mapkkk3* single, or *mapkkk3 yda* double mutant seedlings despite their severe
809 growth/developmental defects. Seeds from Col-0, *mapkkk3*, *yda/+*, and *mapkkk3 yda/+*
810 plants were sterilized and plated on MS plates. Seven days later, seedlings (including
811 the defective *yda* and *mapkkk3 yda* homozygous seedlings) were transferred to liquid
812 culture medium. Fourteen-day-old Col-0, *mapkkk3* single, *yda* single, and *mapkkk3 yda*
813 double mutant seedlings were treated with flg22 (30 nM final concentration) and
814 collected at the indicated time. The phosphorylation activation of MPK3 and MPK6 were
815 detected by using anti-pTEpY antibody. An equal amount of total proteins (10 µg) was
816 loaded in each lane, as confirmed by CBB staining of duplicate gels. (**B**) MPK3/MPK6
817 activation in response to flg22 treatment is partially compromised in the *mapkkk3*
818 *mapkkk5* double mutant seedlings. Fourteen-day-old Col-0, *mapkkk3* single, *mapkkk5*
819 single, and *mapkkk3 mapkkk5* double mutant seedlings were treated with flg22 (30 nM
820 final concentration) and collected at the indicated time. The phosphorylation activation
821 of MPK3 and MPK6 were detected as in (A).

822

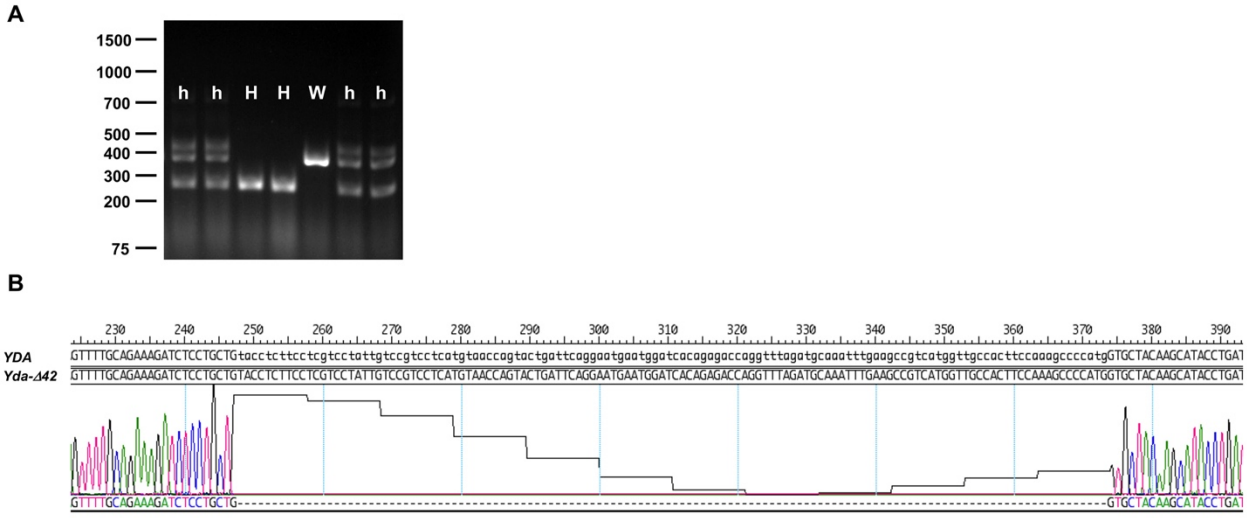

823

824 **Supplemental Figure S3: Genotyping and sequencing identification of *yda-Δ42***
825 **mutant allele generated using CRISPR-Cas9.**
826 (**A**) Representative gel image of PCR genotyping of *yda-Δ42* mutation using primers
827 listed in Supplemental table 1. W: wild type, h: heterozygous, and H: homozygous. (**B**)
828 A 50-µL PCR reaction was run as in (A). After separation on a 2% agarose, the DNA
829 was separated on a 2% agarose gel and then recovered using Zymoclean gel DNA
830 recovery kit. Sequencing was performed using the forward primer listed in
831 Supplemental table 1. Numbers above the sequence indicate the nucleotide number
832 from ATG start codon.
833

834 **Supplemental Table 1. Primers used in this study**

Name	Sequence	Purpose
YDA-F1 genotyping	AGTTTCTCAGGGGCAAATCTCA	*yda* genotyping
YDA-B1 genotyping	CTGAGCAGCTGTAGGACGATTT	
MAPKKK3-F1 caps	TACTTGGTGGGGAAGAAAGTCC	*mapkkk3-2* genotyping
MAPKKK3-B1 caps	CTGATCCAGATGAGCTAACGCT	
MAPKKK5-F1 genotyping	AACTCACGTGTTTAGCCATGC	*mapkkk5-2* genotyping
MAPKKK5-B1 genotyping	CGCGAGATAGTGTTTCCTCAC	
YDA-Cas9-F1	attgGACGAGGAAGAGGTACAGC	For AtU6-26-YDA site 1-sgRNA construct
YDA-Cas9-B1	aaacGCTGTACCTCTTCCTCGTC	
YDA-Cas9-F2	attgGTATGCTTGTAGCACCATG	For AtU6-26-YDA site 2-sgRNA construct
YDA-Cas9-B2	aaacCATGGTGCTACAAGCATAC	
YDA-del-F1 genotyping	GAAACTGGGATTCGCATCTGAG	CRISPR/Cas9 *yda-del* mutant identification and sequencing
YDA-del-B1 genotyping	CCCACAGAACTTCCACTAGACA	

835
836